Real-time FPGA implementation of the DTC Power Control for DFIG-Generators applied to wind turbines

Badre Bossoufi

Laboratory of Electrical Engineering and Maintenance, Higher School of Technology, EST-Oujda,
University of Mohammed I, Morocco.
LISTA Laboratory, Faculty of Sciences Dhar El Mahraz, Sidi Mohamed Ben Abdellah University, Fez,
Morocco
*badre_isai@hotmail.com

Abstract — **In this paper we develops a new control strategy for extracting and controlling the power of the Doubly-Fed Induction Generator (DFIG) applied to wind turbines. A new contribution for the regulation of the active and reactive power is presented, with the aim of an injection to the distribution network. The proposed model in this paper is based on direct torque control (DTC), which is based on performance estimators to improve the quality of the system. The energy quality genered by wind system will be injected into the distribution network according to international standards. Finally, the results of the real-time implementation of the control are implemented on the Matlab / Simulink Xilinx System Generator environment. The entire wind turbine system has been tested in laboratory conditions using the test bench. Simulation and experimental tests show the high dynamic performance and robustness of the proposed control.**

Keywords-   DFIG-Generator,   Direct   Torque   Control, Matlab/Simulink, Wind Turbine.

I. INTRODUCTION

The Renewable energy is clean and inexhaustible. And since other energy sources are expensive, many countries have encouraged researchers to study and develop renewable energy conversion systems (solar energy, wind energy, etc ...). [1] In, fact, renewable is rapidly developing in the world, especially wind power (it is developed by many countries and is experiencing very significant growth + 30% per year on average for 10 years [2-3]).

It is therefore expected that this massive integration of wind generation will cause a disturbance in the functioning of the overall grid. To anticipate these problems, preliminary studies are needed. For this it is necessary to have reliable model of wind generators, both for the conversion process for the command. The electrical configuration of a wind influences functioning. The fact that a wind turbine is fixed speed or variable speed depend example of this configuration. The main advantages of both types of operation are:

✓ In the case of a fixed speed operation:
  - Electrical system simple;
  - Greater reliability; Low probability of excitation of resonant frequencies of the wind turbine elements;

  - No need for electrical control system;
✓ In the case of a variable speed operation:
  - Increase energy efficiency;
  - Reduction of torque oscillations;
  - Reduction of forces to which the power converter;
  - Generation of electric power of a higher quality.

There are still a few years; almost all wind turbines operating at fixed speed. They contained mostly an asynchronous squirrel-cage generator [4,7].

With the use of asynchronous machines, the greater part of the power is directly distributed to the grid by the stator and about 25% of the total power through the power converter through the rotor. This gives the opportunity to use smaller and therefore less expensive converters. The disadvantage of this system is the presence of the rotor blades, which requires a labor increased service. Today, 80% of new wind turbines contain doubly fed induction motors (wound rotor) [8]. For the application in a wind system, a generator operating mode is interesting. Indeed, if the speed variation range does not exceed (±) 30% of that in or beyond the synchronous speed, the machine is capable of delivering a power ranging from 0.7 to 1.3 times the rated power. The converter is then sized to pass only the power of the slip. It is then less bulky, less expensive, requires less heavy cooling system and generates fewer harmonic [6].

In this paper, we present a technique to control two power converters which is based on the DTC control. We analyse their dynamic performances by simulations in Matlab/Simulink environment. We start by modelling of the wind turbine, and then a tracking technique operating point at maximum power point tracking (MPPT) will be presented. Thereafter, we present a model of the DFIG in the dq reference, and the general principle of control of both power converters which is based on DTC technique. Finally, the principle of the implementation on the FPGA target and source program Xilinx System Generator, and the test benchmark for the experimental validation of the proposed model in my lab work.
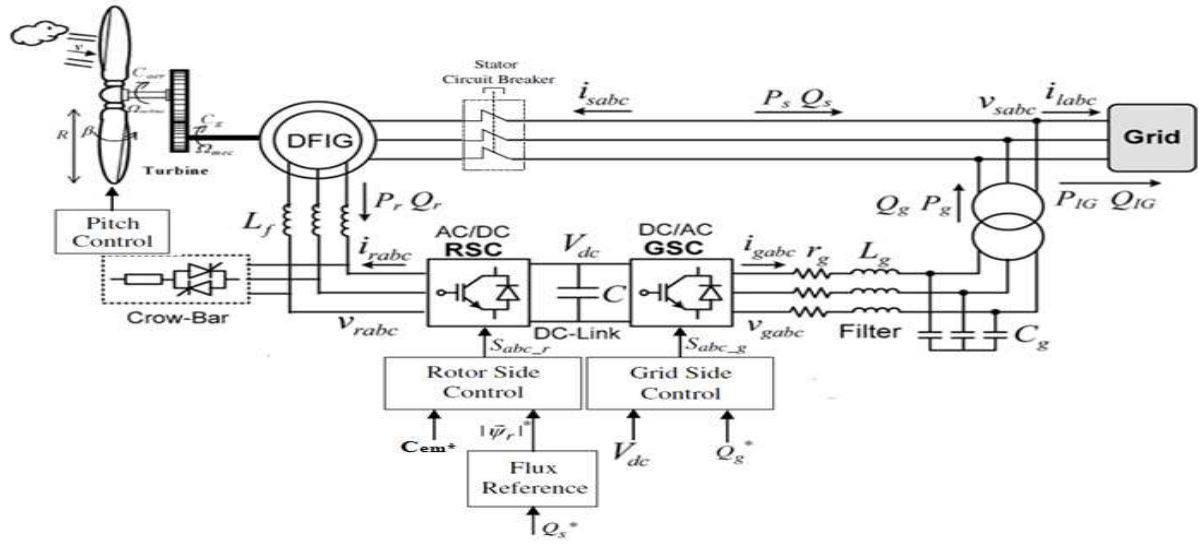
Figure 1.   Architecture of the Control

II. MODELING OF WIND POWER SYSTEM

A. Wind-Turbine model

The model of the turbine is modeled from the following system of equations: [7-8]:

$$P_{incident} = \frac{1}{2}.\rho.S.v^3 \tag{1}$$

$$P_{extracted} = \frac{1}{2}.\rho.S.C_p(\lambda,\beta).v^3 \tag{2}$$

$$\lambda = \frac{\Omega_t.R}{v} \tag{3}$$

$$C_p^{max}(\lambda,\beta) = \frac{16}{27} \approx 0.593 \tag{4}$$

$$C_p(\lambda,\beta) = c_1\left(c_2.\frac{1}{A} - c_3.\beta - c_4\right)e^{-c_5\frac{1}{A}} + c_6.\lambda \tag{5}$$

$$\frac{1}{A} = \frac{1}{\lambda + 0.08.\beta} - \frac{0.035}{1+\beta^3} \tag{6}$$

$$C_{al} = \frac{P_{eol}}{\Omega_t} = \frac{1}{2}.\rho.S.C_p(\lambda,\beta).v^3.\frac{1}{\Omega_t} \tag{7}$$

$$J = \frac{J_{tur}}{G^2} + J_g \tag{8}$$

$$J\frac{d\Omega_{mec}}{dt} = C_{mec} = C_{ar} - C_{em} - f.\Omega_{mec} \tag{9}$$

S : the area swept by the pales of the turbine $[m^2]$
ρ : the density of the air ($\rho = 1.225 kg/m^3$ at atmospheric pressure).
v : wind speed $[m/s]$.
$Cp (\lambda, \beta)$: the power coefficient.
λ : the specific speed
β: the angle of orientation of the blades
Ω_t : Rotational speed of the turbine
J_g : inertia of the generator.
Ω_{mec} : Mechanical speed of DFIG
$c_1 = 0.5872, c_2 = 116, c_3 = 0.4, c_4 = 5, c_5 = 21, c_6 = 0.0085$
The six coefficients c_1, c_2, c_3, c_4, c_5 are modified for maximum Cp equal to 0.564 for $\beta = 0°$.

The *Fig.3* shows the evolution of the power coefficient as a function of λ for different values of β. A coefficient of maximum power of Cp=0.564 is obtained for a speed ratio λ which is (3) (*λopt*). Fixing β and λ respectively to their optimal values, the wind system provides optimal power.
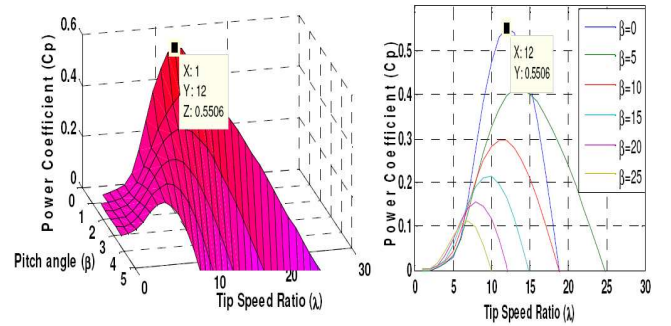

Figure 2.   Curves of the power coefficient

B. DFIG Model System

The equations of the stator voltages Vs (d, q) and the rotor Vr (d, q) of the DFIM in the reference of Park are written as follows: [9, 13]:

Voltages at the stator:

$$\begin{cases} V_{sd} = R_s.i_{sd} + \frac{d\psi_{sd}}{dt} - \omega_s.\psi_{sq} \\ V_{sq} = R_s.i_{sq} + \frac{d\psi_{sq}}{dt} + \omega_s.\psi_{sd} \end{cases} \tag{10}$$

• Voltages at the stator:

$$\begin{cases} V_{rd} = R_r.i_{rd} + \frac{d\psi_{rd}}{dt} - \omega_r.\psi_{rq} \\ V_{rq} = R_r.i_{rq} + \frac{d\psi_{rq}}{dt} + \omega_r.\psi_{rd} \end{cases} \tag{11}$$

With: $\omega_s - \omega_r = p.\omega$

The magnetic equations are expressed by the flux expressions in the reference (d, q).

• Flux at the stator :

$$\begin{cases} \psi_{sd} = L_s.\psi_{sd} + M.i_{rd} \\ \psi_{sq} = L_s.\psi_{sq} + M.i_{rq} \end{cases} \tag{12}$$

• Flux at the rotor :

$$\begin{cases} \psi_{rd} = L_r.\psi_{rd} + M.i_{sd} \\ \psi_{rq} = L_r.\psi_{rq} + M.i_{sq} \end{cases} \tag{13}$$

With: $M = M_{sr} = M_{rs}$

The electromagnetic torque is expressed as a function of the currents and the flows by:

$$\begin{cases} T_{em} = p.\left(\psi_{sd}.i_{sq} + \psi_{sq}.i_{sd}\right) \\ T_{em} = p.\left(\psi_{rq}.i_{rd} - \psi_{rd}.i_{rq}\right) \end{cases} \tag{14}$$

The fundamental equation of dynamics is:

$$T_{em} = T_r + J.\frac{d\Omega}{dt} + f.\Omega \tag{15}$$

With:

$V_{s(d,q)}, V_{r(d,q)}$: Stator and rotor voltages in the reference of Park.

$I_{s(d,q)}, I_{r(d,q)}$: Stator and rotor currents in the reference of Park.

$\psi_{s(d,q)}, \psi_{r(d,q)}$: Stator and rotor flux in the reference of Park.

ω_s, ω_r : Stator and rotor pulsations.

Ω : Mechanical pulsation.

T_{em} : Electromagnetic torque.

Ω : Rotation speed of the machine ($\omega=p.\Omega$).

f : Coefficient of viscous friction.

III. DTC CONTROLLER APPLIED TO DFIG GENERATOR

A. Direct Torque Control principle

The objective of the DTC is the direct regulation of the machine torque by applying the various voltage vectors of the inverter, which determines its state. Controlled variables are: Stator flux and electromagnetic torque which are usually controlled by hysteresis regulators. The aim is to maintain the stator flux quantities and the electromagnetic torque within these hysteresis bands. The output of these controllers determines the voltage vector of the inverter to be applied at each switching instant [11-13]:.

In a DTC control, it is preferable to work with a high calculation frequency in order to reduce the torque oscillations caused by the hysteresis regulators.

The general characteristics of a direct torque control are:
✓ Direct control of torque and flux, from the selection of the switching vectors of the inverter.
✓ Indirect control of stator intensities and voltages.
✓ Obtaining fluxs and stator currents close to sinusoidal shapes.
✓ Dynamic response of the machine very fast.
✓ The existence of the oscillations of the torque which depends, among other things, on the bandwidth factors of the hysteresis regulators.
✓ The switching frequency of the inverter depends on the amplitude of the hysteresis bands.

This method of control has the following advantages:
✓ Do not require calculations in the rotor index (d, q);
✓ There is no PWM voltage modulation calculation block;
✓ It is not necessary to torque the currents from the control voltages;
✓ To have only one regulator, that of the external speed loop;
✓ It is not necessary to know the rotor position angle with great precision because only the information on the sector in which the stator flux vector is located is necessary;
✓ Dynamic response is very fast.

B. Operation and sequences directly applicable on a two-stage voltage inverter

The state of the switches, assumed to be perfect, can be represented by three Boolean control quantities Sj (j = a, b, c) such that:
• Sj = 1 If the top switch is closed and the bottom is open;
• Sj = 0 If the top switch is open and the bottom switch is closed.

We can then write:

$$\overline{V}_s = \sqrt{\frac{2}{3}}.E.\left[S_a + S_b.e^{j\frac{2\pi}{3}} + S_c.e^{j\frac{4\pi}{3}}\right] \tag{20}$$

The various combinations of the three quantities (Sa, Sb, Sc) make it possible to generate eight positions of the vector $\overline{V}_s$, two of which correspond to the zero vector [24-27]:

$$\begin{cases} V_0 = V_7 = 0 \\ V_1 = \sqrt{\frac{2}{3}}.E \\ V_2 = \sqrt{\frac{2}{3}}.E.(0.5 + j\frac{\sqrt{3}}{2}) \\ V_3 = \sqrt{\frac{2}{3}}.E.(-0.5 + j\frac{\sqrt{3}}{2}) \\ V_4 = -\sqrt{\frac{2}{3}}.E \\ V_5 = \sqrt{\frac{2}{3}}.E.(-0.5 - j\frac{\sqrt{3}}{2}) \\ V_6 = \sqrt{\frac{2}{3}}.E.(0.5 - j\frac{\sqrt{3}}{2}) \end{cases} \tag{21}$$
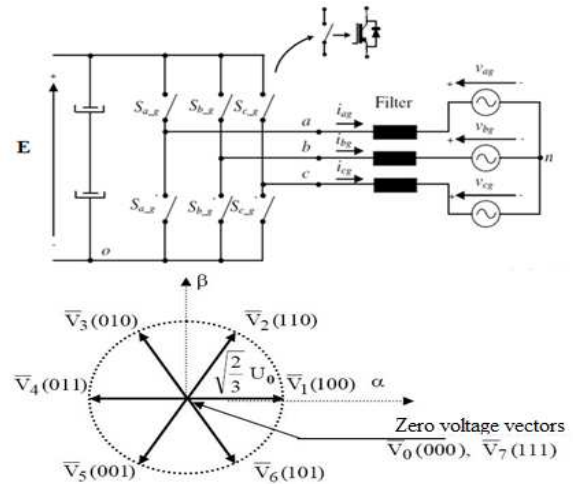

Figure 3. Inverter of voltage and development of tension Vs

C. Principle of Control

1. Stator flux vector control

The Direct torque control is based on the orientation of the stator flux. The expression of the stator flux in the Concordia repository is:

$$\overline{\Phi}_s = \int_0^t (\overline{V}_s - r_s.\overline{I}_s).dt + \overline{\Phi}_s(0) \tag{22}$$

In the case where a non-zero voltage vector is applied during a time interval [0, T], we have: Vs >> Rs Is. Therefore (5.8) can be written:

$$\overline{\Phi}_{s\alpha} \cong \overline{\Phi}_s(0) + \overline{V}_s.T \Rightarrow \Delta\overline{\Phi}_{s\alpha} \cong \overline{V}_s.\Delta t \tag{23}$$

The equation (6.9) implies that the end of the stator flux $\overline{\Phi}_s(t)$ vector moves along a straight line whose direction is given by the voltage vector applied;

It is possible to operate with a module of the flux vector $\overline{\Phi}_s$ which is practically constant, but it should be noted that this is only possible if the control period and therefore the sampling period is very low in front of the flux rotation period.

2. Selecting the voltage vector

The space of evolution of $\overline{\Phi}_s$ in the fixed reference frame (stator) is generally delimited by decomposing this space into six symmetrical zones with respect to the directions of the non-zero voltages. When the flux vector is in the numbered area k, both vectors $\overline{V}_k$ and $\overline{V}_{k+3}$ have the largest flux component. The flux and torque control is ensured by the selection of one of four non-zero vectors or one of the two null vectors
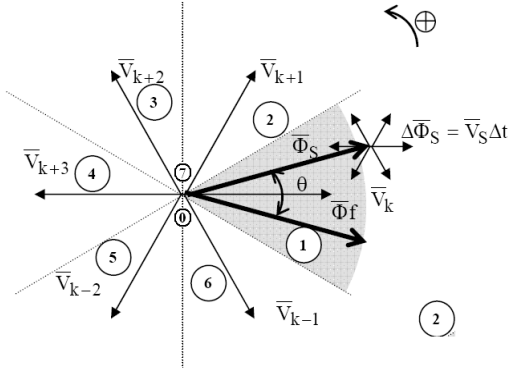

Figure 4.   Space vectors of the inverter and the corresponding variations of the stator flux vector

4. Estimation of the stator flux

The flux estimation can be carried out on the basis of the measurements of the stator current and voltage magnitudes of the machine [30]:

From the equation: $\overline{\Phi}_s = \int_0^t (\overline{V}_s - r_s.\overline{I}_s).dt$

We obtain the components α and β of the flux vector:

$$\begin{cases} \Phi_{s\alpha} = \int_0^t (V_{s\alpha} - r_s.i_{s\alpha}).dt \\ \Phi_{s\beta} = \int_0^t (V_{s\beta} - r_s.i_{s\beta}).dt \\ \Phi_s = \Phi_{s\alpha} + j.\Phi_{s\beta} \end{cases} \quad (25)$$

The voltages Vsα and Vsβ are obtained from the commands (Sa, Sb, Sc), from the measurement of the voltage E by applying the Concordia transform:

$$\begin{cases} V_{s\alpha} = \sqrt{\frac{2}{3}} E \left[S_a - \frac{1}{2}(S_b + S_c) \right] \\ V_{s\beta} = \frac{1}{\sqrt{2}} E (S_b - S_c) \\ \overline{V}_s = V_{s\alpha} + j.V_{s\beta} \end{cases} \quad (26)$$

Similarly, the currents isα and isβ are obtained from the measurement of the actual currents isa, isb and isc (isa + isb + isc = 0) and by applying the Concordia transformation:

$$\begin{cases} i_{s\alpha} = \sqrt{\frac{2}{3}} i_{sa} \\ i_{s\beta} = \frac{1}{\sqrt{2}} (i_{sb} - i_{sc}) \\ \overline{i}_s = i_{s\alpha} + j.i_{s\beta} \end{cases} \quad (27)$$

$$\Phi_s = \sqrt{\Phi_{s\alpha}^2 + \Phi_{s\beta}^2} \quad (28)$$

The area Ni in which the vector $\overline{\Phi}_s$ is situated is determined from the components Φsα and Φsβ. The angle δ between the reference frame the two components of the stator flux $\overline{\Phi}_s$ in the frame (α, β) is equal to:

$$\delta = Arc \tan\left(\frac{\Phi_{s\beta}}{\Phi_{s\alpha}}\right) \quad (29)$$

5. Estimation of electromagnetic torque

The electromagnetic torque can be estimated for all types of synchronous machines from the estimated flux and current quantities.

From their components (α, β), the torque can be put in the form:

$$C_e = p(\Phi_{s\alpha}.i_{s\beta} - \Phi_{s\beta}.i_{s\alpha}) \quad (30)$$

6. Elaboration of the control vector

6.1. Flux corrector

Its purpose is to keep the end of the vector $\overline{\Phi}_s$ in a circular crown as shown in Figure (10). The output of the corrector must indicate the direction of evolution of the module of $\overline{\Phi}_s$, in order to select the corresponding voltage vector. For this purpose a simple two-stage hysteresis corrector is perfectly suited, and also allows to obtain very good dynamic performance.

The output of the corrector is represented by a Boolean variable (Cflx) which directly indicates whether the amplitude of the flux must be increased (Cflx = 1) or decreased (Cflx = 0) so as to maintain:

$$\left| (\Phi_s)_{ref} - \Phi_s \right| \leq \Delta\Phi_s \quad (31)$$

With: (ΦS) ref is the flux set point, and ΔΦS is the hysteresis width of the corrector.
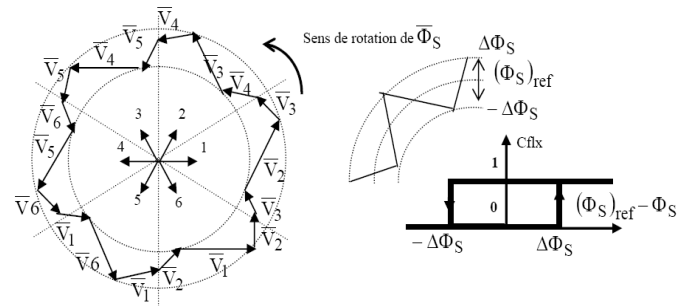

Figure 5.   Hysteresis flux corrector and selection of the corresponding voltage vectors.

6.2. Three-level torque corrector

The function of the torque corrector is to keep the torque within the limits $\left|(C_e)_{ref} - C_e\right| \leq \Delta C_e$, with (Ce) ref the torque reference and ΔCe the hysteresis band of the corrector. However, a difference with the flux control is that the torque can be positive or negative depending on the direction of rotation of the machine. The output of the corrector, presented by the Boolean variable Ccpl (6.7), indicates directly whether the amplitude of the torque should be increased in absolute value (Ccpl = 1) for a positive setpoint and Ccpl = -1 for a negative setpoint or decreased (Ccpl = 0).

This corrector allows a rapid decrease of the torque. For example, one applies the vectors $\overline{V}_{k-1}$ and $\overline{V}_{k-2}$, if one chooses a direction of rotation positive (trigonometric sense). In this case, the flux $\overline{\Phi}_r$ will catch up with the flux $\overline{\Phi}_s$ more quickly because the latter does not merely wait for it (null vectors) but goes to meet it (reversal of the direction of rotation of)

6.3. Development of the control table

Our objective is to perform an efficient control both in steady state and in transient mode, by combining the different switching strategies, to finally develop the most optimal combination based on the mathematical relationships of the spatial vectors, fluxs Stator, rotor flux and current and stator voltage. According to the principle of the DTC structure, the adequate selection of the voltage vector, at each sampling period, is made to maintain torque and flux within the limits of the two hysteresis bands. In particular, selection is made on the basis of the instantaneous flux $\overline{\Phi}_s$ and torque error.

Depending on the sector determined by phase δ of the estimated flux and the evolution of the magnitude of the latter and the evolution of the estimated torque, it is possible to choose the voltage Vs to be applied in order to respect the flux and torque setpoints. We thus have 3 parameters for the choice of the vector $\overline{V}_s$, table 1 makes it possible to choose the appropriate vector.

Table 1 Table of Selection of Voltage Vectors in the Six Sectors

Cflx	Sector k Ccpl	(1) $\delta \in \left[-\frac{\pi}{6}, \frac{\pi}{6}\right]$	(2) $\delta \in \left[\frac{\pi}{6}, \frac{3\pi}{6}\right]$	(3) $\delta \in \left[\frac{3\pi}{6}, \frac{5\pi}{6}\right]$	(4) $\delta \in \left[\frac{5\pi}{6}, \frac{7\pi}{6}\right]$	(5) $\delta \in \left[\frac{7\pi}{6}, \frac{9\pi}{6}\right]$	(6) $\delta \in \left[\frac{9\pi}{6}, \frac{11\pi}{6}\right]$
1	1	V_2(011)	V_3(010)	V_4(110)	V_5(100)	V_6(101)	V_1(001)
1	0	V_0(000)	V_7(000)	V_0(000)	V_7(000)	V_0(000)	V_7(000)
1	-1	V_6(101)	V_1(001)	V_2(011)	V_3(010)	V_4(110)	V_5(100)
0	1	V_3(010)	V_4(110)	V_5(100)	V_6(101)	V_1(001)	V_2(011)
0	0	V_7(000)	V_0(000)	V_7(000)	V_0(000)	V_7(000)	V_0(000)
0	-1	V_5(100)	V_6(101)	V_1(001)	V_2(011)	V_3(010)	V_4(110)

IV. SIMULATION RESULTS

To validate the model proposed for the control of the wind system, it is applied initially to an asynchronous double-powered DFIM motor, in order to check the performances and to configure the control parameters.
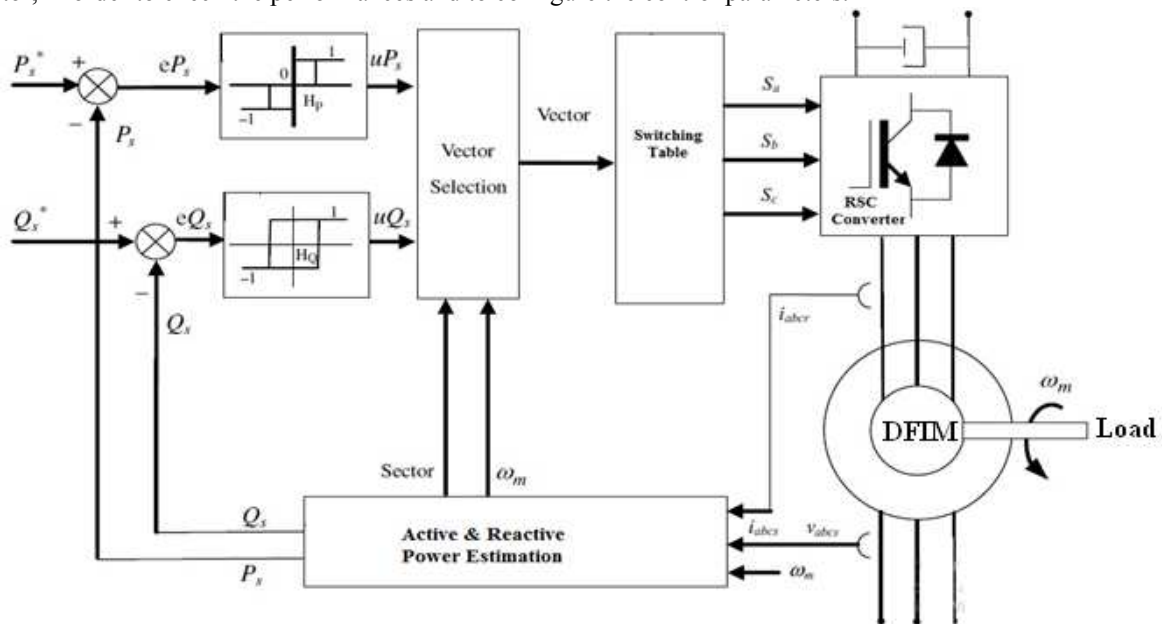

Figure 6. DTC control applied of a DFIM-Motor

The Fig.6 shows in detail the programming of the control shown in Fig.1 (DTC Control) in the SYSTEM GENERATOR environment from Xilinx; we will implement it later in the memory of the FPGA for the simulation of DFIG.

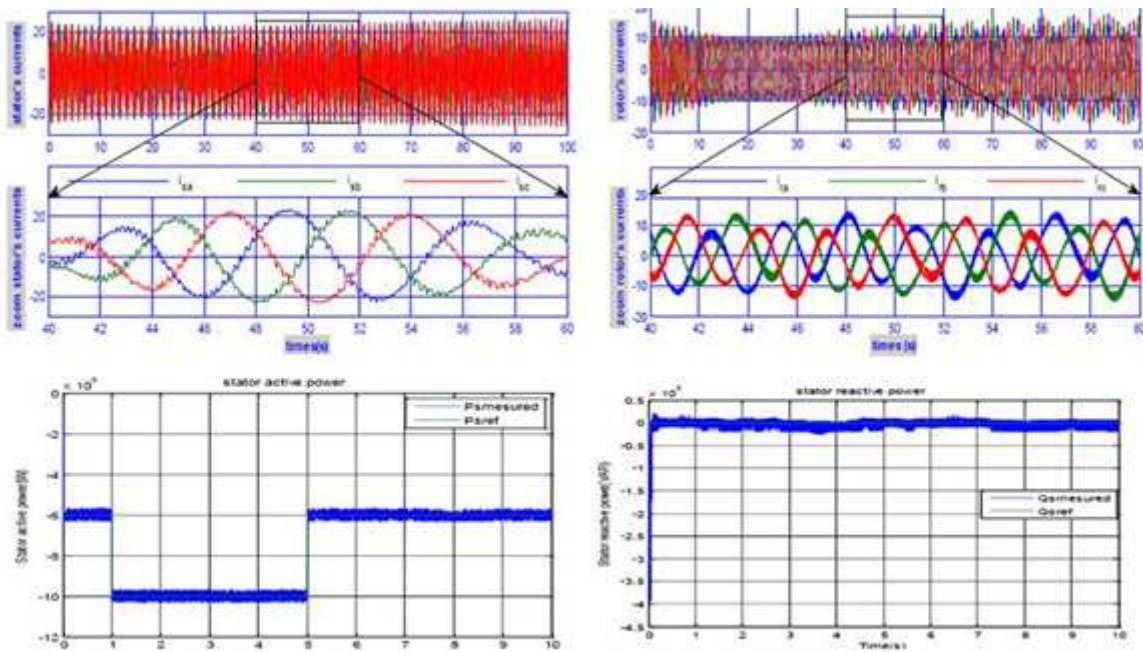Figure 7.   Functional Model DTC from SYSTEM GENERATOR

A. DFIM performances

Figure 8.   DFIM-Motor performance for DTC power control

The figure 8 shows the performance of the system when applying the DTC control. We observe that the rotation speed of the machine follows its reference. The stator module (d, q) is perfectly circular. However, the flux of the rotor undergoes a ripple superimposed on its circular trajectory. The stator and rotor voltages in the frame (a, b, c) and the collections show a sinusoidal shape. Likewise, the stator currents and the currents of the rotor respond well to the variants imposed on the torque and their shape is sinusoidal. However, due to the non-constant switching frequency (use of hysteresis comparators), these currents are rich in harmonics which increase the losses and the drives of acoustic noises and torque oscillations which can excite mechanical resonances.

B. Wind-turbine performances

The wind speed is given as a sum of several harmonics:

$$Vvent = V_0 + \sum_{i=1}^{n} Vi . sin(\omega i . t) \tag{33}$$

The following figure shows the proposed model of the DTC command applied to a MADA motor on the Matlab & Simulink environment:
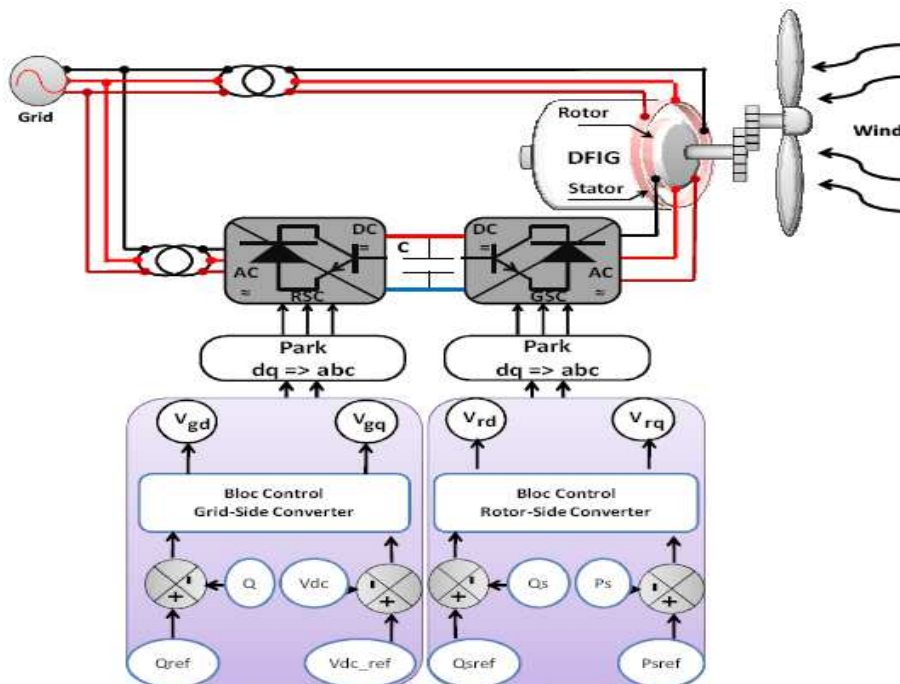

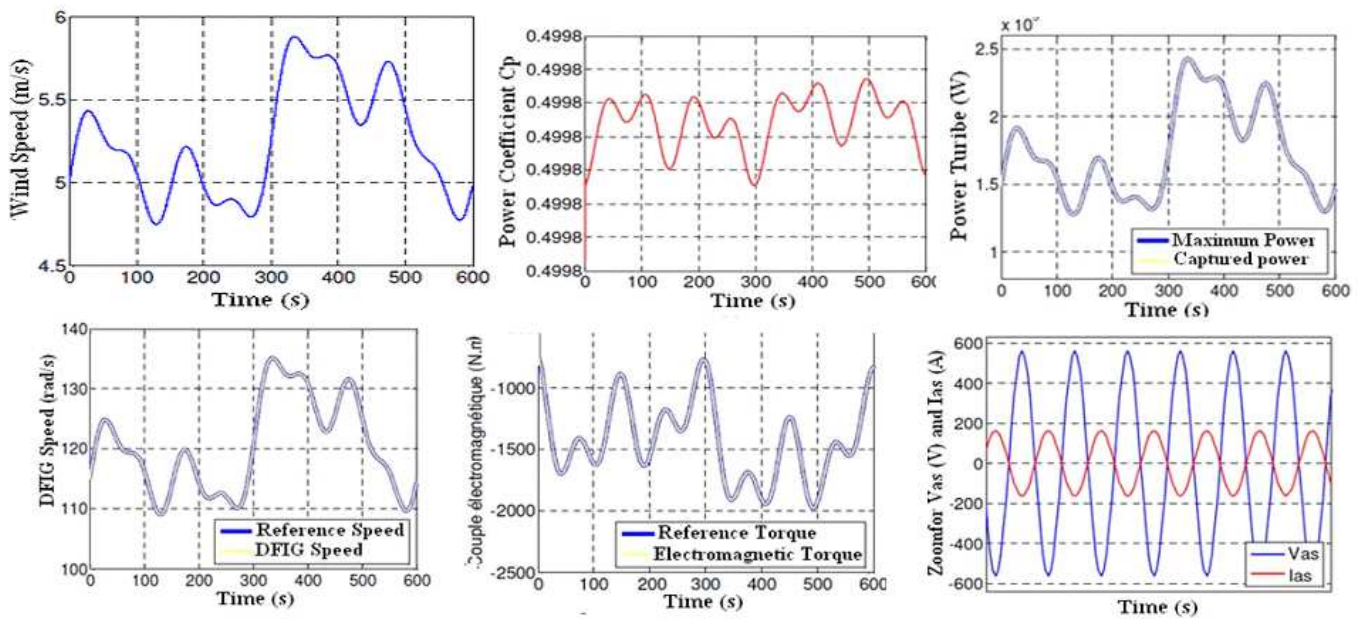Figure 9.   Simulation scheme of adaptive DTC Control applied for DFIG-wind-turbine

Figure 10. The Simulation results of the asynchronous wind generator dual power and stator flux oriented, with a DTC controller

V. EXPERIMENTAL RESULTS

In this work, we are particularly interested in the implementation of the Backstepping command on the FPGA target. We start with a modelling of the wind turbine, and then a study of the technique of tracking the point of operation at maximum power will be presented. Subsequently, we present a model of the MADA in the benchmark dq, and the general principle of the control of the two power converters which is based on the Backstepping command. The principle of the implementation of this command on the FPGA target is studied. Finally, a discussion and interpretation of the results obtained as well as the performances of the FPGA will be spread out. The control of wind turbines based on MADA is tested in the test bench shown in Fig. 11:
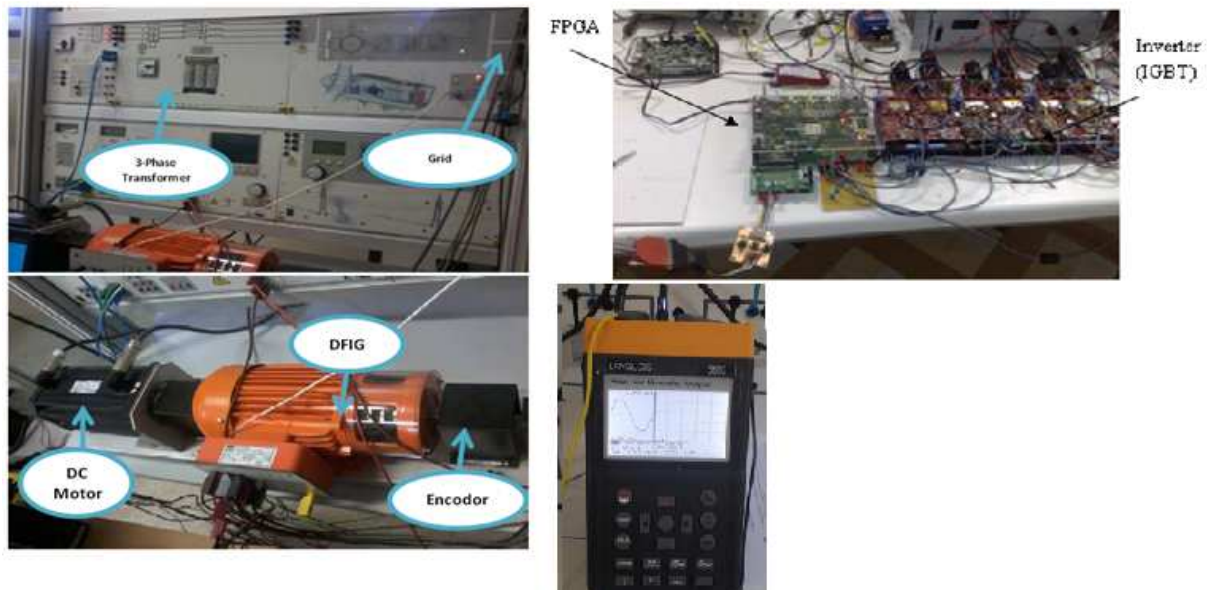

Figure 11. Experimental Benchmark of Wind Turbine System

The experimental bench consists of:
- Control unit for dual-power asynchronous generator wind generator: which enables voltage regulation and synchronization with the distribution network, based on an FPGA board and linked to the MSC and LSC converters
- Three-phase multifunction machine (dual supply generator): has the following characteristics:

Nominal voltage:	400 / 230 V, 50 Hz
Nominal Current:	2,0 A / 3,5 A

Nominal Speed:	1400 / 1500 min-1
Nominal Power :	0,8 kW
cos phi :	0,75
Excitation voltage:	130 V CA / 24 V CC
Excitation current:	4 A CA / 11 A CC

- Three-phase cut-off transformer for wind turbines,
- Incremental position sensor 1024 pulses,
- Servo machine test bench 1 kW,
- Power supply for electrical machines,
- Coupling sleeve 1 kW,

- Coupling protection cover 1 kW,
- Analogue / digital millimeter, power meter and power factor,

In *Fig.12 the* experimental results *DTC* of *PMSM* with the *FPGA* platform are shown. Clearly the constant set values for stator flux linkage magnitude and torque result, because of the hysteresis controllers in the *DTC* scheme, in d-axis and q-axis current components that are bounded within hysteresis limits. The hysteresis control is visible in the stator flux locus plot as well. Update frequency for this implementation is 20 kHz. All results were extracted from the *FPGA* by the ChipScope tool of Xilinx.

A. DFIG performances
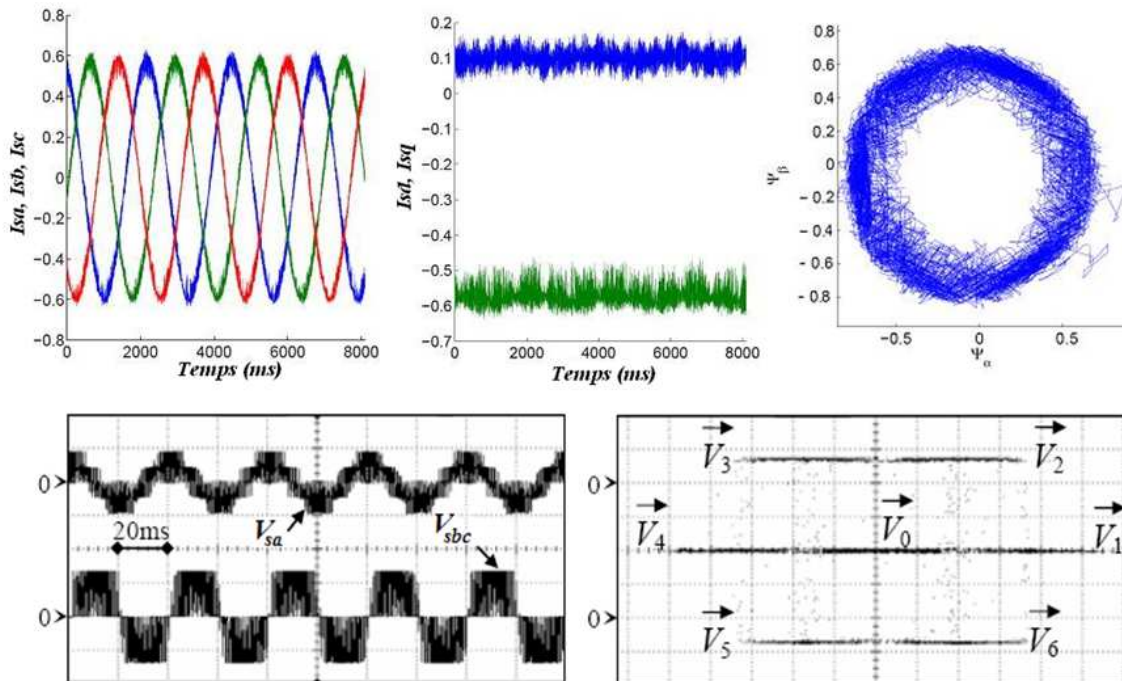
Figure 12. Performances of DFIG

The figures 12 show that the control system satisfies the basic requirements of the control strategy and therefore validates the correct functionality of the system. In fact, it can be noted that:

• The switching frequency is limited to the sampling frequency of the control algorithm to ensure proper operation of the semiconductors on the power devices.

• The switching frequency increases slightly when the vector magnitude of the stator current decreases.

Implementing the DTC command on the FPGA target has the following disadvantages:

- The switching frequency is variable. It is limited to half the sampling frequency of the control algorithm and a maximum at very low speed.

- The voltage vectors at zero are not applied.

At the hardware level, the execution time of the control architecture is of the order of a few microseconds, which allows a better control of the currents, including a low harmonic distortion rate.

B. Wind-turbine performances

Using the reduced model, we applied a profile closer to the evolution of the real wind was filtered to suit the slow dynamics of the system studied random wind. The objective is to see the degree of continuing point of maximum power and efficiency of the speed control provided by the DTC controller.
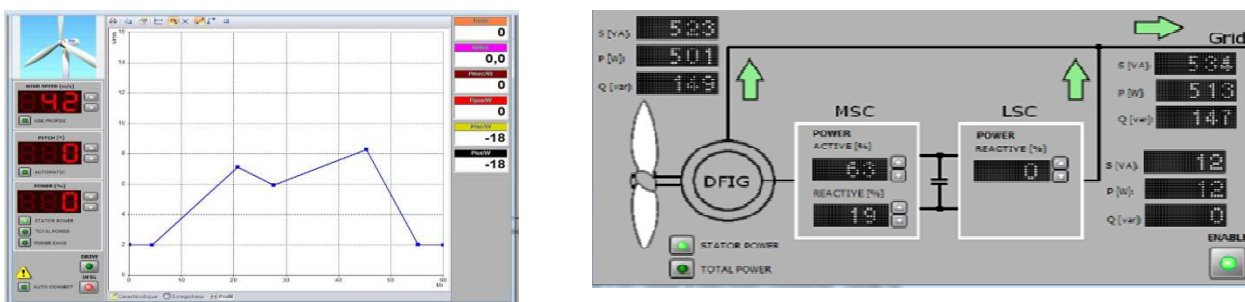

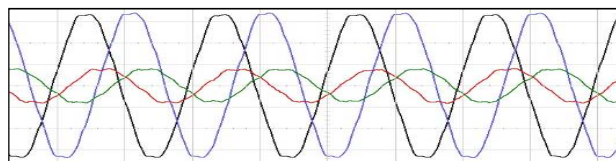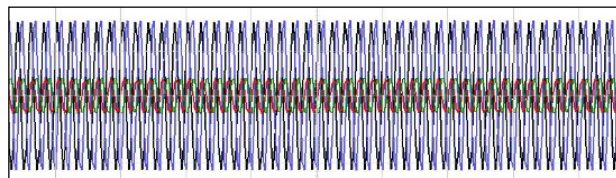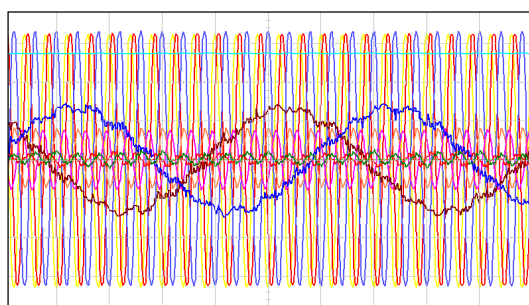Figure 13. Profile in software WindSim of Wind Speed

Figure 14. General profile of the voltages and currents in the plan "abc", Profile of Grid voltage and current and Zoom Grid voltage and current
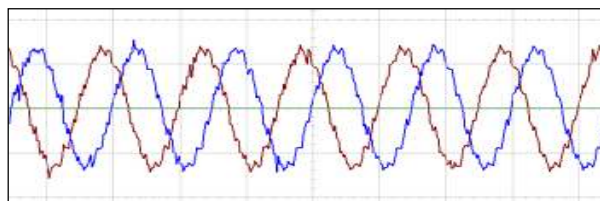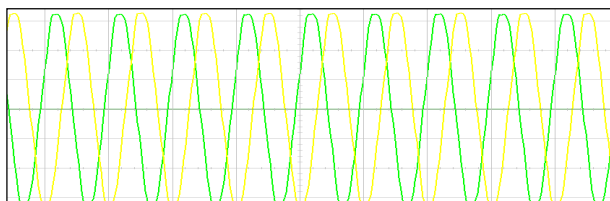

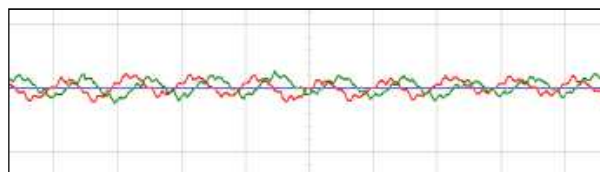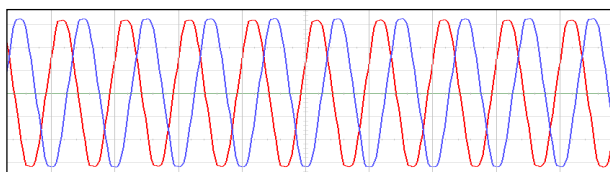Figure 15. Profile of the stator: (a) stator voltage , (b) Stator current

Figure 16. Profile of the Rotor: (a) Rotor voltage , (b) Rotor current

The analysis and interpretation of the results obtained show the robustness and the validation of the proposed control for the wind systems based on the DFIG.

- The voltages and currents at the outputs of the system are purely sinusoidal with a constant frequency and do not present any problems when connecting to the grid.
- The active and reactive powers are sent to the electrical grid, we notice that almost reactive power is zero, which makes the system more robust.
- The DFIG is in hyper-synchronous generator mode. The rotor's power is sent to the grid with the power's stator.

Our approach is an additional contribution to the implementation of non-linear controls of wind systems based on the DFIG. The results obtained show the reliability and robustness of the proposed control to inject power in the electrical grid.

VI. CONCLUSION

This work has been devoted to modeling, simulation and analysis of a wind turbine operating at variable speed. A stable operation of the wind energy system is obtained with the application of nonlinear DTC control. The overall operation of the wind turbine and its control system were illustrated by responses to transient and permanent control systems.

Generator supplied power to the grid network with an active power whatever the mode of operation. The wind generator has been tested and modeled with a variable speed operation for a power of 200 W. Simulation results show that the proposed wind system and is feasible and has many advantages.

VII. REFERENCES

[1]   T. Ackermann and Soder, L. « An Overview of Wind Energy-Status 2002 ». Renewable and Sustainable Energy Reviews 6(1-2), 67-127 (2002).

[2]   T. Burton, D. Sharpe, N. Jenkins and E. Bossanyi, *Wind Energy Handbook.* John Wiley&Sons, Ltd, 2001.

[3]   W. L. Kling and J. G. Slootweg, « Wind Turbines as Power Plants». in Proceeding of the IEEE/Cigré workshop on Wind Power and the impacts on Power Systems, 17-18 June 2002, Oslo, Norway.

[4]   D. Seyoum, C. Grantham, «Terminal Voltage Control of a Wind Turbine Driven Isolated Induction Generator using Stator Oriented Field Control». IEEE Transactions on Industry Applications, pp. 846-852, September 2003.

[5]   X. YU, K. STRUNZ, « Combined long-term and shortterm access storage for sustainable energy system », 2004 IEEE Power Engineering Society General Meeting, vol.2, pp.1946-1951, 10 June 2004.

[6]   X. YAO, C. YI, D. YING, J. GUO and L. YANG, « The grid-side PWM Converter of the Wind Power Generation System Based on Fuzzy Sliding Mode Control », Advanced Intelligent Mechatronics, IEEE 2008, Xian (Chine).

[7]   B.Bossoufi, M.Karim, A.Lagrioui, M.Taoussi, A.Derouich "Observer Backstepping control of DFIG-Generators for Wind Turbines Variable-Speed: FPGA-Based Implementation" *Renewable Energy Journal (ELSIVER),* pp 903-917, Vol. 81. September 2015.

[8]   G. Poddar and V. T. Ranganathan, "Direct Torque and Frequency Control of Double- Inverter-Fed Slip-Ring Induction Motor Drive," IEEE Trans. Ind. Electron.,Vol. 51, No. 6, pp. 1329–1337, December 2004.

[9]   G. Poddar and V. T. Ranganathan, "Sensorless Double-Inverter-Fed Wound-Rotor Induction-Machine Drive," IEEE Trans. Ind. Electron., Vol. 53, No.1, pp. 86–95, February 2006.

[10] J. Dai, D. Xu, and B.Wu, "A Novel Control Scheme for Current-Source-Converter-Based PMSG Wind Energy Conversion Systems," IEEE Trans. Power Electron., Vol. 24, No. 4, pp. 963–972, April 2009.

[11] H. Akagi and H. Sato, "Control and Performance of a Doubly-Fed Induction Machine Intended for a Flywheel Energy Storage System," IEEE Trans. Power Electron., Vol. 17, No. 1, pp. 109–116, 2002.

[12] A. K. Jain and V. T. Ranganathan, "Wound Rotor Induction Generator With Sensorless Control and Integrated Active Filter for Feeding Nonlinear Loads in a Stand-Alone Grid," IEEE Trans. Ind. Electron., Vol. 55, No. 1, pp. 218–228, January 2008.

[13] G. Sarwar Kaloi, J. Wanga, M. Hussain Baloch," Active and reactive power control of the doubly fed induction generator based on wind energy conversion system" Journal of Elsevier of Energy Reports, pp. 194-200, Vol.02, November 2016.